Journal of
NANOSTRUCTURES
JNS
NANOSTRUCTURES
JNS.kashanu.ac.ir

Fabrication, and Effect of Reflux time on Structural Properties of Pure and Al-Doped TiO_2 Nano-rod

Mehran Riazian*

Department of Engineering, Tonekabon branch, Islamic Azad University, Tonekabon, Iran.

Article history:
Received 12/12/2012
Accepted 17/4/2013
Published online 1/6/2013

Keywords:
Nanorod
TiO_2
Aluminum
Dopant

**Corresponding author:*
E-mail address:
m.riazian@toniau.ac.ir
Phone: 98 912 2116905
Fax: +98 192 4271105

Abstract

TiO_2 nanorods can be used as dye-sensitized solar cells and as various sensors and photocatalysts. These nanorods are synthesized by a using thermal corrosion process in a NaOH solution at 200 ^oC with TiO_2 powder as a source material. In the present work, the synthesis of TiO_2 nanorods in anatase, rutile and Ti_8O_{15} phases and the synthesis of TiO_2 nanorods by using the sol-gel method and alkaline corrosion to incorporate aluminum oxide dopant are reported. The morphologies and the crystalline structures of the TiO_2 nanorods are characterized using field emission scanning electron microscope (FE-SEM), atomic force microscope (AFM), and X-ray diffraction (XRD) techniques.

1. Introduction

TiO_2 is an important material that is used in many industrial applications related to photo-splitting of water [1], photocatalysis [2], photovoltaic devices [3], *etc*. It is known to have three natural polymorphs, i.e, rutile, anatase, and brookite. The photocatalytic performance of this compound depends on the characteristic of the TiO_2 crystallites, such as the size and surface the area. Therefore, modifications of its physical and chemical properties are of interest to researchers [4-9]. One possible way to modify the properties of TiO_2 crystallites is by adding a second semiconductor into the TiO_2 matrix. Dopants, such as silica or alumina, which exists as discrete particles at the nanocrystal interfaces and "pins" the grain boundaries in place by restricting surface diffusion and reducing the radius of curvature of the TiO_2 nanocrystals [10, 11]. Many studies addressing both with TiO_2 doping with different metals and the synthesis and characterization of one-dimensional (1D) nanostructures (nanowires, nanotubes, nanorods) have received considerable attention due to unique properties and novel applications of these nanostructures [12-15].

Many methods have been successfully developed for the fabrication of 1D nanostructures, including vapor-solid, vapor-liquid-solid and solution-liquid-

solid template-based synthetic approaches and laser ablation [16-21]. However, almost all of these methods use either catalyst materials or physical templates, which unavoidably bring some contamination to the products. Therefore, one has to explore a new approach to synthesize 1D nanomaterials without using preformed templates or catalysts. The sol-gel process is employed quite often for the synthesis of nanosize catalytic materials. The incorporation of an active metal in the sol during the gelation stage allows the metal to have a direct interaction with the support.

In the present work, first, a TiO_2 nanorod is synthesized by using a hydrolysis procedure in simple wet chemical approach with titanium tetra isopropoxide. Beside the pure samples, it is doped into the aluminum matrixes. The obtained results indicated the nanorod properties depend on the preparation procedures and the reflux time.

2. Experimental procedure

The synthesis of TiO_2 nanorods and doped TiO_2 nanorods in sol-gel method are reported [4, 22, 23]. The composition of the starting solution and the experimental conditions used for the TiO_2 nanorods are listed in Table 1. Fig. 1 illustrates the preparation procedures. The precursors, ATSB Aluminium tri-sec-butylate (Merck), titanium tetra isopropoxide (TTIP) ($Ti(OPr^i)_4$, Merck), 0.1 N nitric acid (Merck, Ethanol (Merck) and distilled water are used without further purification.

The starting point for the synthesis of a targeted system is a solution prepared by mixing the precursors: In detail, according to the molar ratio in Table 1. Precursors are chosen (TTIP, deionized water, ethanol). ATSB is dissolved in 20 cc of deionized water and stirred at room temperature (RT) for 48 h to get a solution of pH=5. Then, for precipitation, ammonia solution is added dropwise so that pH=8 and is then centrifuged at 1500 rpm to gather the precipitate. The precipitate is heated at 50 ^{0}C for 24 h. For the formation of a rod shape the powders are immersed in 10 N NaOH solution in a teflon balloon at 200 ^{0}C in 6 and 12 h. Once more, the powders are gathered with a centrifuge and are purified with 0.1 N nitric acid and distilled water to eliminate the Na ions.

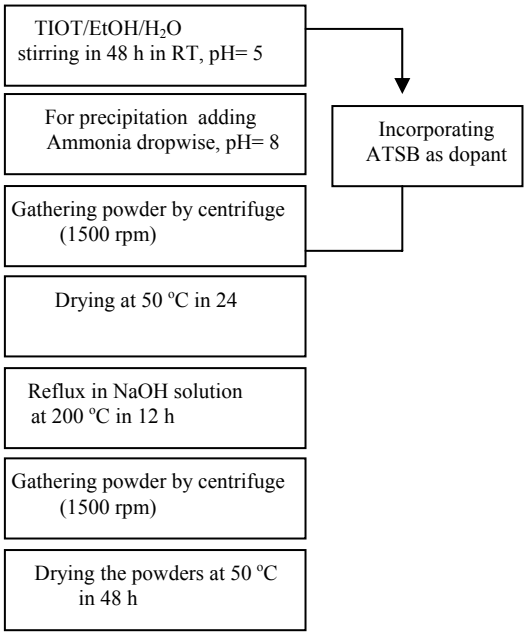

Fig. 1. Schematic flowchart illustrating the steps in the synthesis pathway of TiO_2 nanorods.

Table 1. Composition of starting solutions and experimental conditions for TiO_2 nanorods preparation.

Method used	Method step	Precursor	Molar ratio(MR)	Stirring Time (h)	pH
Alkoxide route	1	TTIP	TTIP /EtOH/H_2O =1:0.022/	24	5
		ATSB	TTIP / ATSB =87.3		
	2	Precipitation with Ammonia	Dropwaise	0.5	8

XRD patterns measured on a (GBC-MMA 007 (2000)) X-ray diffractometer. The diffractograms recorded with copper 0.02^o step size in which the

speed 10o/min) radiation over a 2θ range of 10°–80°. Transmission electron microscopy (TEM) (CM10 Philips) used to investigate the structure and morphology of the nanorods. Field-emission electron microscopy (FE-SEM) (S-4160 Hitachi) used to investigate the morphology of the nanoparticles. AFM (Easy Scan 2 Flex (Switzerland), silicon tip used. The measurements made at 20 °C and relative humidity of 45%. FT-IR measurements performed on a 1730 Infrared Fourier Transform Spectrometer (Perkin-Elmer) using the potassium bromide as the background.

3. Results and discussion

The crystallographic phases of the composite ceramic are investigated by using the XRD technique, and the results are shown in Figs. 2 and 3. As shown in this figure, different crystalline phases are formed. Fig. 2 also shows partly amorphous structure for pure sample due to the short range ordering of the network [15, 19, 24 , 25]. The characteristics of the XRD peaks are summarized in Tables 2 and 3. The grain size values are calculated from the Scherrer equation:

$$r = \frac{0.9\lambda}{2\beta\cos\theta}, \quad (1)$$

where λ = 0.154 nm, β is the full width at half maximum (FWHM), and θ is the reflection angle. Data in Table 3 shows the influence of the reflux time on the grain size of different phases. Precursor chemistry, experimental conditions and the presence of a dopant material influence the nucleation and the growth of the different polymorphs of TiO_2 [26, 27].

The averages of the nanocrystalline sizes are calculated based on Scherrer's formula. In the doped state, the crystallite sizes are bigger than the pure state. With increasing the reflux time, the nanocrystallne sizes of anatase and rutile phase increased and, Vice versa, the nanocrystallne size of Ti_2O_3, Al_2O_3 and AlO_2H decreased.

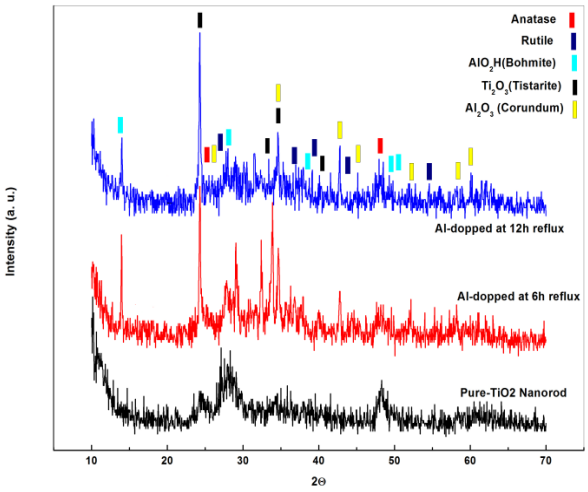

Fig. 2. XRD patterns of pure TiO_2 nanorod and Al doped with 6 h and 12 h reflux time.

Table 2. The 2θ angle, d-space, Miller indexes, grain size of pure TiO_2 nanorod.

Pure state			
Crystalline Phase	**As-prepared**		
	2Θ	**d-space (Å)**	**size (nm)**
Anatase			
Tetragonal	25.33	3.51	11
a=3.8040			
c=9.6140			
Rutile			
Tetragonal	27.55	3.23	7
a=4.5940			
c=2.9590			
Ti_2O_3			
Hexagonal	33.2	2.69	4
a=5.1490			
c=13.6420			
Ti_8O_{15}			
Hexagonal	29.10	3.06	4
a=4.8440			
c=13.2700			

Table 3. The 2θ angle, d-space, Miller indexes, grain size of pure TiO_2 nanorod.

Crystalline Phase	Doped state					
	6 h reflux time			12 h reflux time		
	2Θ	d-space(Å)	size(nm)	2Θ	d-space(Å)	size(nm)
Anatase Tetragonal a=3.8040 c=9.6140	25.15	3.53	7	25.44	3.49	9
Rutile Tetragonal a=4.5940 c=2.9590	27.70	3.21	5	27.60	3.22	25
Ti_2O_3 Hexagonal a=5.1490 c=13.6420	24.33	3.65	47	24.32	3.65	45
AlO_2H Orthorhombic a=2.8678 b=12.2188	13.94	6.36	66	13.95	6.33	26
c=3.6941	34.76	2.57	26	34.69	2.58	14
Al_2O_3 Hexagonal a=4.8440 c= 13.2700						

Lattice strain (ε) of nanocrystallites in the pure and the doped TiO_2 nanorods are determined of the dependence of FWHM (Full Width Half Maximum) on diffraction lines observed in 2θ range of $10\text{-}80^0$ on sinθ according to the Williamson-Hall's equation [28].

$$\beta \cos\theta = \frac{k\lambda}{L} + 4\varepsilon \sin\theta, \quad (2)$$

where β is FWHM observed, shape factor k is assumed to be 0.9 similar to Scherrer equation's. λ is a wavelength of copper radiation (0.154056 nm). The plots of βcosθ against 4sinθ for different samples are approximated to be linear. Lattice strain is determined from the slope of this linear relation. Because of lowly-crystallized powder samples, the linearity between βcosθ and 4sinθ is not very evident [29]. The plots of βcosθ against 4sinθ for different diffraction lines are illustrated in Fig. 3. For low calcination temperature the experimental points for the diffraction lines measured scattered because the peaks are weak and broad so that their FWHMs are difficult to be measured. As it can be seen in Fig. 3, in the pure state the lattice strain is 0.804. With increasing the reflux time from 6 h to 12 h, the lattice strain increases from 0.893 to 1.369 in Al-doped state.

FE-SEM (S-4160 Hitachi) is routinely used to investigate the morphology of the nanoparticles. FE-SEM images of TiO_2 nanorods are shown in Fig. 4 (a). The pure sample has a spherical cover but contains many rods. Nanoparticles seem to be formed in a thin rope shape.

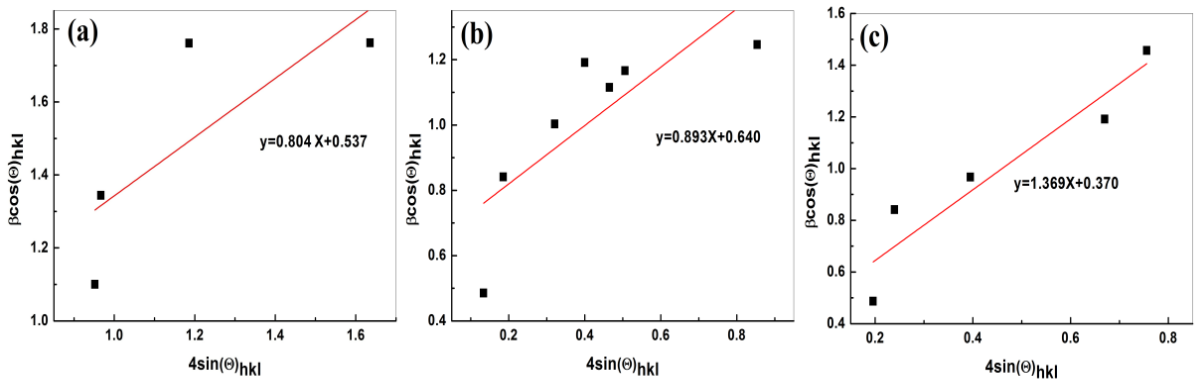

Fig. 3. FE-SEM images of TiO_2 nanorods in (a) pure state (b) doped state with 6 h reflux and (c) 12 h reflux.

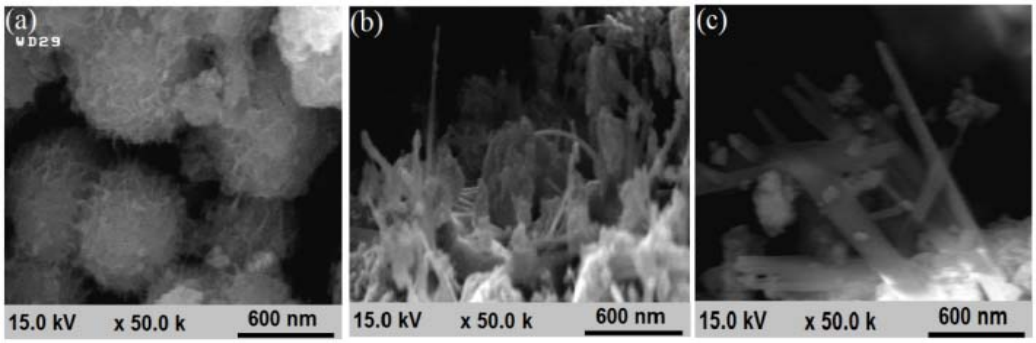

Fig. 4. FE-SEM images of TiO_2 nanorods in (a) pure state (b) doped state with 6 h reflux and (c) 12 h reflux.

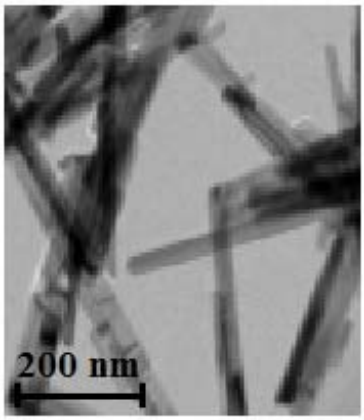

Fig. 5. TEM image of nanorod structure of pure sample.

Figs. 4 (b) and (c) show FE-SEM of TiO_2 nanorods doped with aluminum with 6 h and 12 h reflux time, respectively. The dopants affect the length and the shape in such a way that they enlarge the length and separate the nanorods.

Fig. 5 shows nanorod structure of pure sample. As shown in this figure, the diameter is 43 nm and the length is 400 nm.

The surface morphologies of the TiO_2 nanorods and the TiO_2 nanorods doped with aluminum oxide are presented in Fig. 6. As shown in these figures, the islands have quite compact shapes with lengths of 2 to 3.5 μm in the pure state and about 10 μm in the doped state. After the islands to be as an arm-like shape, the growth seems to continue in a dendritic or irregular pattern while maintaining an arm width of about 6 μm. Two issues affect the rod structures: (1) Because of diffusion of adatoms into the matrix at higher concentrations, a larger fraction of the deposited TiO_2 or dopants impinges onto existing islands.

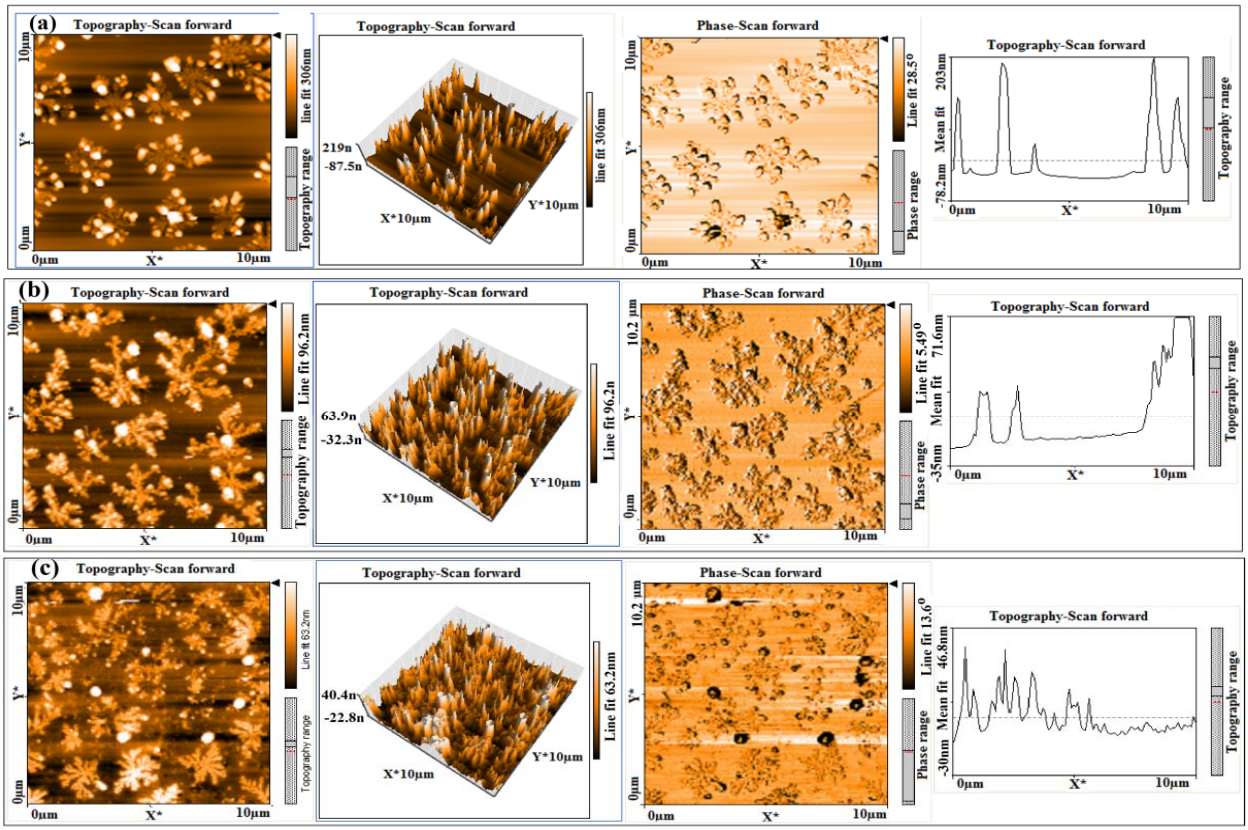

Fig. 6. (a) AFM images of pure TiO_2 nanorods pure state. (b) doped state with 6 h reflux time and (c) doped state with 12 h reflux time.

These adatoms can diffuse off the first islands and condense at the step edge, thereby thickening the structure. (2) Fractals are formed where nanoaggregates shapes have been formed. As the linear size of the islands becomes larger, higher percentages of the TiO_2 or dopants make up the fractal regions between the arms. The TiO_2 or the dopants atoms in these regions tend to fill in the fractal regions and do not contribute to further radial growth. The radial growth, on the other hand, is slowed to the extent that the islands have not coalesced and can still be identified as individual entities. The dendritic shapes are due to a kinetic limitation existing at room temperature, which can be concluded from their thermal instability [30], as shown in Fig. 6.

AFM (Easy Scan 2 Flex, Switzerland) with a silicon tip is used. The measurements are made at 20 ^{0}C and 45% relative humidity. The surface morphologies are characterized by using the average thickness of the sheets, the intervals between the sheets, and roughness parameters such a S_a, S_m and S_q shown in Table 5. The parameter S_a is the roughness average $S_a = \frac{1}{N}\sum_{l=0}^{N-1}|Z(x_l)|$. S_m is the mean value $S_m = \frac{1}{N}\sum_{l=0}^{N-1} Z(x_l)$. The parameter S_q is the root-mean-square value $S_q = \sqrt{\frac{1}{N}\sum_{l=0}^{N-1}(Z(x_l))^2}$. As can be seen in Fig. 6 and table 4, the roughnesses of the doped surfaces of the TiO_2 nanorods are greater than there of the pure TiO_2 nanorods and the roughnesses increase with increasing the reflux time.

Table 4. Roughness parameter of TiO_2 nanorods.

Sample	S_a (nm)	S_q (nm)	(pm)
pure TiO_2 nanorods in figure 6 (a)	34.979	54.599	5.987
doped TiO_2 nanorods in figure 6 (b)	37.021	49.139	5.898
DopedTiO_2 nanorods in figure 6 (c)	54.153	64.903	63.48

FT-IR measurements are performed on a 1730 Infrared Fourier Transform Spectrometer (Perkin-Elmer) with potassium bromide as the background. The FTIR spectra of TiO_2 nanorods are recorded in the wave number range of 400-4000 cm^{-1} (Fig. 7). In the prepared gel, the 3200 cm^{-1} band has to be attributed to hydroxyl groups from water and ethanol, which are occluded in the titania pore. The OH bending band of water in the gel is observed at 1650 cm^{-1}, and in the low-energy region, the Ti-O band is found at 1061 and below 1000 cm^{-1}. The FT-IR spectra show peaks characteristic of Ti-O-Ti (495–436 cm^{-1}). A comparison between pure nanorods and doped nanorods indicates that the bands at 780 and 570 cm^{-1} can be to the Al-O vibration bond.

4. Conclusion

The homogeneous hydrolysis of metal alkoxide and corrosion with NaOH provided an excellent technique to prepare TiO_2 nanorod materials. Experimental results indicated that the homogeneous hydrolysis of tetra isopropy ortho titanate via the sol-gel route is a promising technique for preparing photosensitive material with uniform nanoparticles. In this study, nanocrystalline TiO_2 nanorod particles were successfully synthesized by using a chemical method and a heat treatment process. The phase transformation of titanium dioxide depends on the dopants and the reflux time.

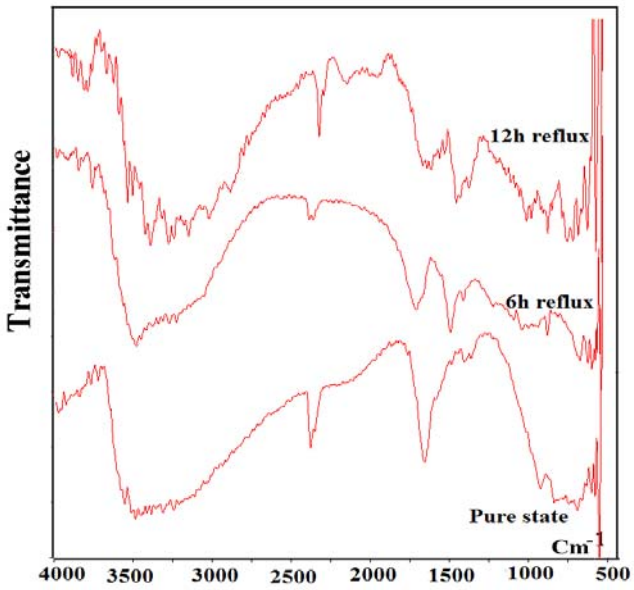

Fig. 7. FTIR spectra of pure and Al-doped TiO_2 nanorods with 6 h reflux time and 12 h reflux time.

The addition of other oxides such as aluminum affected the structural properties, such as the size, strain and activation energy. In the doped state, with increasing the reflux time, the nanocrystallne size of anatase and rutile phase increased and Vice versa, the nanocrystallne size of Ti_2O_3, Al_2O_3 and AlO_2H decreased. The lattice strain increased in Al-doped state. With increasing the reflux time from 6 h to 12 h, the lattice strain increased. The roughnesses of the doped surfaces of the TiO_2 nanorods were greater than there of the pure TiO_2 nanorods and the roughnesses increased with increasing the reflux time. FTIR spectra of the ternary composite was presented and showed the possible bonds Ti-O, Ti-O-Ti, Ti-OH, and Al-O.

Acknowledgment

The authors thank Islamic Azad University, Tonekabon branch for financial support through a research project.

References

[1] A. Y. Kim, M. Kang, Int. J. Photoenergy. 10 (2012) 1155-1164.

[2] H. F. Lai, C. C. Chen. , J. R. Wu, S. C. Lu, J. Chinese Chemical Soc. 59 (2012) 78-89.

[3] A. Loiudice , A. Rizzo , L. D. Marco , M. R. Belviso, G. Caputo, P. D. Cozzoli, J. Phys. Chem. 21 (2012) 3987-3995.

[4] M. Riazian, A. Bahari, , Pramana J. Phys. 78 (2012) 319-331.

[5] M. Riazian, A. Bahari, Int. J. Physical Sci. 6 (2011) 3756-3767.

[6] M. Riazian, N. Montazeri, E. Biazar, Oriental J. Chem. 27 (2011) 903-910.

[7] A. Bahari, M. Riazian, Int. J. Nano Dimensions. 3 (2012) 127-139.

[8] D. N. Gupta, K. R. Sahu, I. Das, A. De, U. De, Indian J. Phys. 84 (2010) 1413-1429.

[9] M. R. Vaezi, S. K.Shendy, T. J. Ebadzadeh, Indian J. Phys. 86(2012) 9-13.

[10] L. A. O'Dell, S. L. P. Savin, A. V. Chadwick, M. E. Smith, Nanotechnology. 16 (2005) 1836-1843.

[11] A. V. Chadwick, S. L. P. Savin, L. A. O'Dell, M. E. Smith, J. Phys.: Condens. Matter. 18 (2006) 163-170.

[12] N. Iguchi, C. Cady, R. Snoeberger, B. Hunter, E. Sproviero, C. Schmuttenmaer, R. Crabtree, G. Brudvig, V. S. Batista, Physical Chemistry of Interfaces and Nanomaterials VII, Proc. Of SPIE 70340, 2008.

[13] Y. Xie, H. Qian, Y. Zhong, H. Guo, Y. Hu, Int. J. Photoenergy. 10 (2012) 682138-10.

[14] R. Jayasinghe, A. G. Unil Perera, Y. Zhao, Bull. American Phys. Soc. 57 (2012) 93-109.

[15] J. Qiu, F. Zhuge, Xn. Li, X. Gao, X. Gan, L. Li, B. Weng, Z. Shi, Y. Hwae, J. Mat. Chem. 22 (2012) 3544-3549.

[16] M. A. Pugachevskii, Phys. Astronomy. 38 (2012) 328-331.

[17] H. Wang, Y. Liu, Z. Liu, H. Xu, Y. Deng, H. Shen, Cryst. Eng. Comm., 14 (2012) 2278-2282.

[18] E. J. Schwalbach, S. H. Davis, P. W. Voorhees, J. A. Warren, D. Wheeler, J. Applied Phys. 111 (2012) 24302-10.

[19] S. R. Gajjela, C. Yap, M. Grätzel, P. Balaya, Energy Environ. Sci. 3 (2011) 838-845.

[20] S. Mitra, A. Mandal, S. Banerjee, A. Datta, S. Bhattacharya, A. Bose, D. Chakravorty, Indian J. Phys. 85 (2011) 649-666.

[21] H. Rath, S. Anand, M. Mohapatra, P. Dash, T. Som, U. P. Singh, N. C. Mishra, Indian J. Phys. 83 (2009) 559-565.

[22] M. Raizian, S. D. Rad, R. Ramezani, J. Phys. Soc. 62 (2013) 459-468.

[23] M. Riazian, Indian J. Phys. accepted (2013) DOI 10.1007/s12648-013-0323-3.

[24] B. Prasai, B. Cai, M. K. Underwood, J. P. Lewis, D. A. Drabold, J. Mater. Sci. 12 (2012) 6439-6445.

[25] Q. Li, B. Liu, L. Wang, D. Li, R. Liu, B. Zou, T. Cui, G. Zou, Mater. Sci. 900 (2012) 1823-1828.

[26] J. G. Li, T. Ishigaki, X. Sun, J. Phys. Chem. C. 111 (2007) 4969-4976.

[27] A. Pottier, C. Chaneac, E. Tronc, L. Mazerolles, J. P. Jolivet, J. Mater. Chem. 11 (2001) 1116-1121.

[28] A. K. Zak, W. H. Majid, M. E. Abrishami, R. Yousefi, Solid State Sci. 13 (2011) 251-256.

[29] M. Inagaki, R. Nonaka, B. Tryba, A. W. Morawski, Chemosphere. 64 (2006) 437-444.

[30] J. Ivancoa, T. Haberb, J. R. Krenna, F. P. Netzera, R. Reselb, M. G. Ramseya, Surf. Sci. 601 (2007) 178-187.